

# THE INTERNATIONAL JOURNAL OF SCIENCE & TECHNOLEDGE

## Heat Transfer Analysis of Cavity Absorber in LFRSC System – A Review of CFD Approach

**Dr. R. Manikumar**

Assistant Professor/School of Mechanical and Manufacturing Engineering,  
Addis Ababa Science and Technology University, Addis Ababa, Ethiopia

**Dr. A. Valan Arasu**

Associate Professor, Department of Mechanical Engineering,  
Thiagarajar College of Engineering, Madurai, India

### **Abstract:**

*The Linear Fresnel Reflector Solar Concentrator (LFRSC) system is one of the basic solar equipment through which solar energy is converted into thermal energy with the help of heat transfer fluid which flows through the absorber. A detailed review of the literature that deals with the numerical analysis in the design of absorber is presented. Most of the researchers used Computational Fluid Dynamics (CFD) as a numerical simulation tool for modeling the absorber. CFD uses powerful computer and applied mathematics, to model fluid flow situations for the prediction of heat and momentum transfer of the flow processes. The quality of the solutions obtained from CFD simulation is largely within the acceptable range as compared to experimental values proving that CFD is an effective tool for predicting the behavior and performance of an absorber. In most of the reviews, a modern CFD code ANSYS FLUENT version is used to simulate heat transfer and fluid flow through a conventional absorber of LFRSC system. The review is performed in a thematic way in order to allow an easier comparison, discussion and evaluation of the findings obtained by researchers related to modeling of the absorber which affects the performance of LFRSC system.*

**Keywords:** Cavity absorber, LFRSC, computational fluid dynamics, overall heat loss coefficient, concentrated radiation

### **1. Introduction**

Due to global warming, an emphasis has been placed on the provision of energy from renewable sources. Whilst renewable energy source can take many forms, solar energy has emerged as the most promising and reliable source available. Solar energy can be harnessed via direct conversion to electricity (photovoltaic) or by using solar steam generation to supply steam to a conventional steam power cycle. Linear Fresnel reflector is one type of the solar concentrator systems which is used for hot water production as well as steam generation. The linear concentration is the technology where the concentration can be done on a line, as in the case of parabolic trough collector. With the reflectors aligned in the North-South direction, a simple orientation, perpendicular in the East-West direction bring back the image concentration of the sun on the absorber tubes laid out on the focal line of the concentrator. The LFRSC field can be imagined as a broken-up parabolic trough reflector, but unlike parabolic troughs, it does not have to be of parabolic shape. The parabola is reconstituted roughly using flat fixed mirrors (called as concentrator) whose slope will be fixed according to the noon position of the sun. These fixed reflectors (generally the number varies from 10 to 50), redirect the radiation towards the absorber.

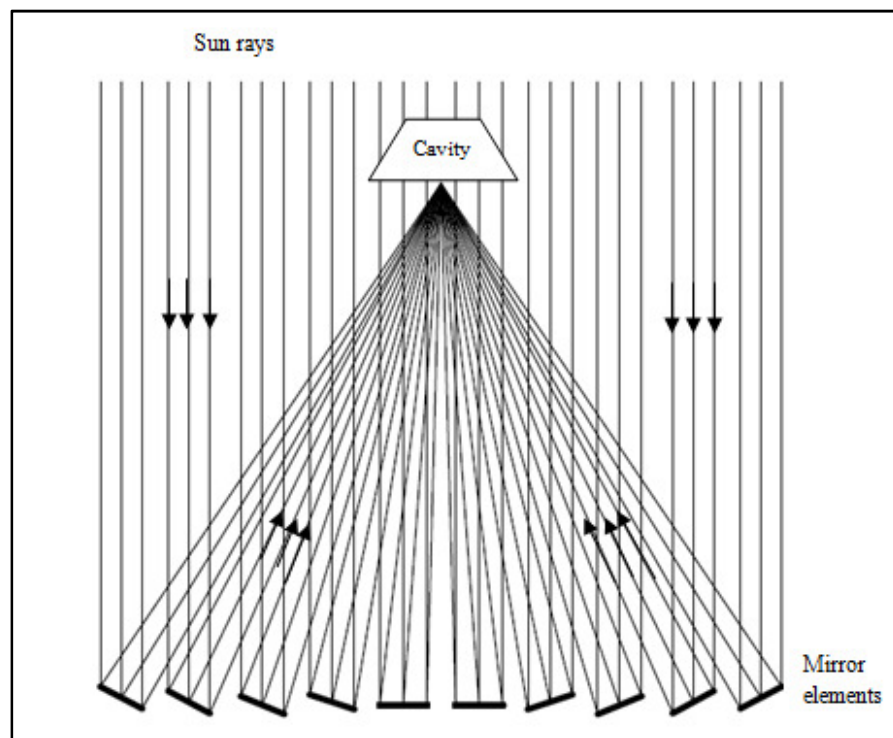


Figure 1: Schematic diagram of LFRSC System

One of the most important roles in the LFRSC system performance is played by the absorber [1-4]. The absorber is nothing but a stationary linear cavity, usually square, rectangular, and trapezoidal, consisting of a number of tubes. The inside of the cavity, external to the tubes contains air which is not in contact with ambient. The tubes are heated by absorbing reflected solar radiation from the LFRSC (Fig. 1) field placed at the ground [5]. The water flowing through the tubes inside the cavity absorbs heat and thereby generates steam inside the tubes. Heat loss from the absorber occurs by a complex mechanism that includes radiation, convection and conduction modes. Knowledge of the heat loss through the structure surrounding the absorber tubes is very important because it affects the efficiency of the collecting system. In operation, the absorber tubes in the considered cavity heat up due to the incident concentrated solar radiation. As it does so, it emits long wave length radiation into the cavity and the absorber tubes. This radiation results in heat loss from the tubes. The emitted radiation is absorbed by inner cavity walls and glass cover at the bottom, which in turn raises their temperature. The resulting temperature gradients lead to natural convection within the cavity, which lead to convective losses from the tubes. Conduction through the cavity walls represents the third mode of heat loss. The cavity receiver heat loss processes involve radiation, convection and conduction heat transfer, and interaction of these three modes makes it difficult to develop a purely analytical model [6]. Because of its relevant influence on the system performance, the heat loss of the absorber was subject of research by several methods, including analytical, numerical simulation using CFD and experimental methods [7-9].

CFD is a science that can be helpful for studying heat transfer, fluid flow and chemical reactions etc., by solving mathematical equations with the help of numerical analysis [10]. CFD employs a very simple principle of resolving the entire system in small cells or grids and applying governing equations on these discrete elements to find numerical solutions regarding pressure distribution, temperature gradients and flow parameters in a shorter time at a lower cost by reducing the required experimental work [11-16]. A lot of experimental studies have been carried out to evaluate performance of absorbers but very few attempts of CFD investigation have been made so far due to complexity of flow pattern and computational limitations. CFD has been greatly developed over recent years, mostly due to the rapid advance in computer technology. It is now possible to solve scientific problems in complex geometries easily using the same techniques. One of the great challenges in the design of a cavity absorber using CFD approach is the selection of appropriate model with exact boundary conditions. In this review, a CFD investigations and its usage for the design of a cavity absorber carried out by the various researchers are presented.

## 2. Thermal Performance of Absorber

The generalized thermal analysis of a concentrating solar collector is similar to that of a flat plate collector [17]. It is necessary to derive appropriate expression for the overall heat loss coefficient  $U_l$ , considering the heat loss between the absorber surface and the transparent bottom glass cover (called as depth of the cavity absorber) and from the transparent cover to the surroundings, neglecting the side plate loss. For the estimation of heat loss coefficient, standard heat transfers relations for glazed surfaces have been used in various literatures [1,5 & 6].

The LFRSC can be imagined as a broken-up parabolic trough reflector [18] and thermal analysis is carried out as similar to the parabolic trough reflector. The working fluid water, which is to be heated in the absorber, has a mass flow rate  $m$ , specific heat  $c$ , an inlet temperature  $T_{fi}$ , an outlet temperature  $T_{fo}$  and ambient temperature  $T_a$ . The glass cover which is placed below the absorber has

been made of a material which is highly transparent to incoming reflected solar radiation and at the same time, opaque to long wavelength re-radiation emitted by the absorber surface. Glass with low ferric oxide content satisfies these requirements [17] and it can be used for the analysis. The one-dimensional analysis has been performed along the direction of fluid flow with the objective of determining the variation of fluid temperature. This analysis will help in linking the useful heat gain rate with the fluid inlet temperature. Consider the control volume, an elementary length  $dy$  of one tube (Fig. 2). As per the first law of thermodynamics, rate of change of enthalpy of the fluid flowing through the control volume is equal to rate of heat transfer to fluid inside the control volume.

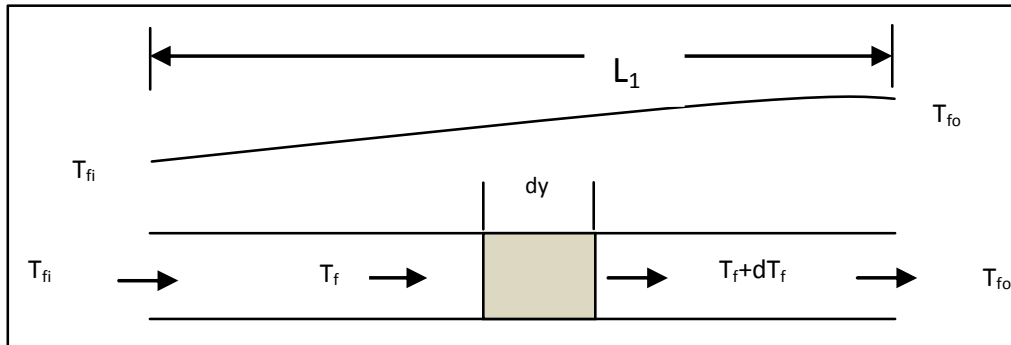


Figure 2: Variation of fluid temperature in flow direction

Thus [17],

$$\left(\frac{m}{N}\right)cdT_f = \frac{1}{N}dq_u = P_i F' [S - U_l(T_f - T_a)]dy \quad (2.1)$$

$$\frac{dT_f}{dy} = \frac{P_i F' U_l}{(m/N)c} \left[ \left( \frac{S}{U_l} + T_a \right) - T_f \right] \quad (2.2)$$

Integrating and using the inlet condition  $y=0$ ,  $T_f = T_{fi}$ , we obtain the temperature distribution,

$$\frac{\left(\frac{S}{U_l} + T_a\right) - T_f}{\left(\frac{S}{U_l} + T_a\right) - T_{fi}} = \exp\left\{-\frac{F' U_l y L_w}{mc}\right\} \quad (2.3)$$

where,  $L_w$  is the width of the absorber plate.

The fluid outlet temperature  $T_{fo}$  is obtained by substituting  $T_f = T_{fo}$  and  $y = L_1$  in the above equation. By simplifying the Equations (2.1) to (2.3), the useful heat gain rate for the concentrator will be obtained.

Heat transfer in the trapezoidal cavity absorber from hot absorber surface (Fig. 3) is mainly through convection and radiation. The trapezoidal cavity absorber is insulated (with glass wool) from three sides to reduce heat loss, there would be heat loss from the absorber through conduction from insulated sides and it is considered as negligible in most of the present simulation models [7-9]. The natural convection type heat transfer occurs inside the cavity. The radiation heat exchange between the hot absorber surface and the glass cover plate of the cavity absorber may be taken as the heat transfer between two infinite parallel surfaces [1] with different surface temperatures. Estimation of the overall heat loss coefficient ( $U_l$ ) of the cavity absorber is done by considering convection and radiation losses from the absorber surface (either plate or tube surface) through glass cover at bottom portion [19].

$$\frac{1}{U_l} = [1/(h_{cp} + h_{rp}) + (A_p / A_c) \{1/(h_{co} + h_{ro})\}] \quad (2.4)$$

The heat loss between the absorber surface and inner glass surface can be estimated by considering heat loss between two horizontal parallel surfaces (hot surface up and cold plate at bottom). The convection heat transfer correlations can be given as [20],

$$Nu_{cp} = 0.163Gr^{0.196} \left(\frac{D_e}{W}\right)^{0.316} \quad (2.5)$$

Physical properties of air have been taken at the average temperature of bottom glass cover and absorber surface temperature. Similarly heat loss at outer cover surface ' $h_{co}$ ' can be estimated by [17],

$$h_{co} = 8.55 + (2.56 * V_w) \quad (2.6)$$

where  $V_w$  is the velocity of wind in m/s.

Radiation losses from a body mainly depend upon body temperature and surface emissivity. Radiation heat transfer coefficient between hot absorber surface and glass cover ( $h_{rp}$ ) can be calculated considering radiative heat transfer modeled as that between two parallel planes [21],

$$h_{rp} = [\sigma(T_p^2 + T_c^2)(T_p + T_c)] / [(1/\epsilon_c) + (1/\epsilon_p) - 1] \quad (2.7)$$

Radiation heat transfer coefficient ( $h_{ro}$ ) from bottom glass cover of the cavity absorber to the ambient can be calculated as [22],

$$h_{ro} = \sigma\epsilon_c(T_c^2 + T_a^2)(T_c + T_a) \quad (2.8)$$

The heat loss coefficient by above method is estimated by using experimental values of absorber surface temperature ( $T_p$  or  $T_s$ ), cover temperature ( $T_c$ ) and ambient temperature ( $T_a$ ). The thermal efficiency ( $\eta$ ) is calculated from,

$$\eta = mc(T_o - T_i) / IA_a \quad (2.9)$$

### 3. Method of Performance Analysis

There are three basic approaches or methods that can be used to solve a problem of fluid flow and heat transfer. These methods are,

- 1) Experimental
- 2) Analytical or Theoretical
- 3) Numerical or Computational (CFD)

#### 3.1 Experimental method:

The most reliable information about a physical process is often given by actual measurement. An experimental method involving full-scale equipment can be used to predict how identical copies of the equipment would perform under the same conditions. Such full scale tests are not possible all the times, because of its expensive [10]. The alternative then is to perform experiments on small scale models. The resulting information however must be extrapolated to full scale, and general rules for doing this are often not available. Further, the small-scale models do not always simulate all the features of the full-scale equipment, because frequently, important features such as combustion or boiling are omitted from the model tests. This further reduces the usefulness of the small scale results. Finally, in many situations, it is serious difficult to measure the readings, and also the measuring instruments are not free from errors [23].

#### 3.2 Analytical method

An analytical prediction works out based on the consequences of a mathematical model, rather than those of real physical model. For the physical processes of interest, the mathematical model mainly consists of a set of differential equations. If the methods of classical mathematics are to be used for solving these equations, there would be little hope of predicting many phenomena of practical interest. In the theoretical approach simplifying assumptions are used in order to make the problems accountable [24].

#### 3.3 Numerical Method

Inside the cavity absorber, heat transfer processes involve all the three modes (radiation, conduction and convection), and the interaction of these makes it quite complicated to carry out a numerical analysis. CFD has been greatly developed over recent years, mostly due to the rapid advance in computer technology. It is now possible to solve scientific problems in complex geometries easily using the same techniques. CFD codes are structured around the numerical algorithms that can tackle fluid flow and heat transfer problems. In order to provide easy access to their solving power, all the commercial CFD packages include sophisticated user interfaces to input problem parameters and to examine the results. Natural convection inside the cavity and thermal radiation between surfaces are modeled and simulated by using ANSYS package with FLUENT software. The present CFD simulation is based on the simultaneous solution of the system of flow and heat transfer equations describing mass, momentum, energy, pressure and radiation. The derived form of the equations can be expressed as [25],

Continuity equation:

$$\frac{\partial(\rho_f u)}{\partial x} + \frac{\partial(\rho_f v)}{\partial y} = 0 \quad (2.10)$$

Energy equation:

$$\rho_f C \left( u \frac{\partial T}{\partial x} + v \frac{\partial T}{\partial y} \right) = u \frac{\partial P}{\partial x} + \frac{\partial}{\partial y} \left( k_a \frac{\partial T}{\partial y} \right) + \mu \left( \frac{\partial u}{\partial y} \right)^2 \quad (2.11)$$

Momentum equation:

$$\rho_f \left( u \frac{\partial u}{\partial x} + v \frac{\partial u}{\partial y} \right) = - \frac{\partial P}{\partial x} + \frac{\partial}{\partial y} \left( \mu \frac{\partial u}{\partial y} \right) \quad (2.12)$$

Equation of state:

$$P = \rho_f RT \quad (2.13)$$

Radiation equation:

$$I = \frac{\sigma T^4}{\pi} (1 - \epsilon^{-as_p}) + I_o \epsilon^{-as_p} \quad (2.14)$$

The above equations are used to solve the steady flow, laminar, natural convection and radiation model considering Boussinesq and non-Boussinesq approximation theories [26]. For the radiation exchange between the internal surfaces of the trapezoidal cavity absorber along with natural convection model, surface to surface option can be chosen [26 & 27] in the numerical procedure. This is used to account for the radiation exchange in an enclosure of gray-diffuse surfaces. The energy exchange between two surfaces depends on their size, separation distance and orientation. These parameters are accounted for by a geometric function called a “view factor”. The main assumption of the absorber model is that, any absorption, emission or scattering of radiation can be ignored. The energy flux leaving in a given surface is composed of directly emitted and reflected energy. The reflected energy flux is dependent on the incident energy flux from the concentrator, which can be expressed in terms of the energy flux leaving all other surfaces. The energy reflected from absorber surface can be expressed as [25],

$$q_o = \epsilon \sigma T_p^4 + (1 - \epsilon) q_i \quad (2.15)$$

#### 4. Applications of CFD in Analyzing Cavity Absorber

One of the most important roles in the LFRSC system performance is played by the cavity absorber [1]. Knowledge of the heat loss through the structure surrounding the absorber tubes is very important because it affects the efficiency of the collecting system. The heat loss depends on several factors, as the geometry of the cavity, materials, insulation thickness, infrared emissivity of the absorber surface, concentration ratio, etc., [27]. Because of its relevant influence on the system performance, the heat loss of the absorber was subject of research by several methods, including analytical simulation, numerical simulation using CFD and experimental methods [1, 6 & 7]. The cavity absorber models are reviewed and discussed.

##### 4.1 Cavity Absorber Modeling

In operation, the absorber surface heats up due to the incident concentrated solar radiation. As it does so, it emits long-wave radiation into the cavity. This radiation represents a heat loss from the absorber surface and results in a decrease in thermal efficiency of the collector [28]. In addition, the emitted radiation is absorbed by the cavity sides and bottom glass cover, which in turn heat up. This promotes buoyancy-driven flows within the cavity, resulting in convection losses and a further reduction in the thermal efficiency. Conduction of heat away from the absorber surface via the sidewalls represents a third mode of a heat loss to be considered [29]. A number of studies have been conducted in the area of heat transfer in cavities by natural convection combined with radiation. The typical cases are square, rectangular and trapezoidal cavity with differentially heated side walls and adiabatic top and bottom surfaces. Kim & Viskanta [30] investigated the combined radiation and natural convection in a rectangular cavity and incorporated wall conduction into their study. They demonstrated that wall conduction has the effect of reducing convection heat transfer in the cavity, as does by the radiation exchange between the surfaces. Nakamura & Asako [31] conducted a numerical and experimental study on the effect of a partition, which has zero thickness and located vertically at the midpoint of the differentially heated cavity. It was found that the emissivity of the top and bottom walls only slightly affect the heat transfer by convection in both cases of conductive and insulated top and bottom walls. On the other hand, the emissivities of the cold and hot walls and of the partition were shown to considerably modify the convective heat transfer. Fusegi & Farouk [32, 33] used a radiatively participating medium in their computational and experimental work on a square cavity. Behina et al [34] have studied the combined radiation and natural convection in a rectangular cavity filled with a non-participating fluid. One wall of the cavity is an isothermal heat source while the opposite wall is allowed to transfer heat to the surroundings via convection and radiation. The two end walls are adiabatic. They concluded that external convection weakens the internal convection, while radiation strengthens the flow. Balaji & Venkateshan [35] have numerically investigated natural convection combined with surface radiation for rectangular cavities of varying aspect ratio (ratio between width of the top surface of the cavity and depth of the cavity) filled with a nonparticipating (transparent) medium. The cavities consisted of differentially heated side walls with adiabatic top and bottom surfaces. They found that for aspect ratio greater than or equal to 2, the convection and radiation mechanisms of heat transfer can be decoupled, and based on this finding, they developed separate correlations for the convection Nusselt number and the radiation Nusselt number.

Tong & Koster [36] numerically studied 2-D natural convection in water with density inversion in a rectangular cavity using finite element model. Non-Boussinesq parabolic density – temperature relationship was incorporated in the model. It was found that interactive convection across the density inversion is dependent on aspect ratio and Rayleigh number. Several experimental and numerical results have been presented to explain the phenomenon of combined natural convection and surface radiation in a closed cavity using various numerical simulation methods. In these aspects, Balaji & Venkateshan [37] numerically investigated the combined surface radiation and free convection in a square cavity with air as the intervening medium. Separate Nusselt number correlations have been developed for both free convective and radiative heat transfer for the Grashof number range of  $10^3$ - $10^6$ . Mlaouah et al [38] numerically investigated the behavior of transitional thermally driven flow in a two-dimensional differentially heated square cavity filled with a gas in cases where the temperature difference increases. Cheng & Muller [39] performed numerical and experimental investigations on natural air convection coupled with thermal radiation in a vertical rectangular channel with one-side heated wall using the CFD code FLUTAN. Based on the experimental and numerical results, the semi-empirical Nusselt number correlation was developed for turbulent natural convection coupled with thermal radiation. Ramesh & Venkateshan [40] have experimentally studied heat transfer by natural convection combined with surface radiation in a square enclosure filled with a nonparticipating medium. Differentially heated side walls and adiabatic top and bottom surfaces were employed. They demonstrated

that natural convection is suppressed in the presence of surface radiation. Correlations for convection Nusselt number and radiation Nusselt number were presented and discussed.

Mezrhab & Bchir [41] studied the effects of adding a thick partition located vertically close to the hot wall of a differentially heated square cavity, forming a narrow vertical channel in which the flow is controlled by vents at the bottom and the top of the partition. It is shown that radiation has a significant influence on the flow and heat transfer in the channel. Han & Baek [42] numerically studied natural convection of a radiating fluid in a rectangular enclosure, with two incomplete adiabatic thin partitions (one on the top and the other at the bottom) under a large temperature difference. They have used the Finite-Volume Method (FVM) to solve the radiative transport equation, and have found that the radiation alters significantly the flow patterns and the thermal distributions. In addition, the surface radiation was dominant over the gas radiation and the results were affected by the baffle configuration. Vierendeels et al [43] computed the solutions for two dimensional, laminar, steady state natural convection of a gas in a square cavity with large temperature differences. Non-Boussinesq and low-Mach number approximation was employed in the simulations. Mezrhab et al [44] presented a numerical study, based on a finite volume method and a boundary element approximation, of the radiation-natural convection interactions in a differentially heated square enclosure, within which a centred, squared, heat-conducting body generates heat. They found that the streamlines and isotherms structures in the enclosure are strongly affected by the thermal radiation heat transfer. Moreover, this one increases considerably the total heat transfer in the enclosure, and allows a good cooling of the body that generates heat. Bouali et al.[45] studied numerically the effects of surface radiation and inclination angle on heat transfer and flow structures in an inclined rectangular enclosure with a centered inner body.

#### 4.2. Trapezoidal Cavity Absorber Modeling

Trapezoidal cavity absorber is one of the promising absorber used in the LFRSC system [46]. The various numerical simulation techniques used by researchers to analyze the heat losses inside the trapezoidal cavity are discussed in the following section.

Correlations for heat transfer analysis inside the absorber have been proposed by Gungor & Winterton [47], and their set of correlations, in the form given by Stephan [48] was the correlations used by both Odeh [49] and by David Reynolds [50] in their earlier work. Liu & Winterton [51] gave a newer correlation that their claim is slightly better than that of Gungor & Winterton [52]. A correlation of Kandlikar [53], as given by John Lienhard et al [54], is the correlation used, as its form is simpler, and it is recommended for use by Kothandaraman & Subramanyan [55]. Bruce Stewart & Burton Wendroff [56] gave some details about the advanced transient two-phase flow models used in the nuclear industry. These models have a mathematical property that, as written, they are 'ill posed'. This means that they cannot be solved without some modification to the problem. A variety of approaches are used, including semi-implicit integration methods, and higher-order finite difference schemes that have the result of adding enough numerical diffusion to the problem that it becomes well-posed and can then reliably be integrated. The detail required in solar thermal energy applications is not as great as that required in nuclear engineering. The problem of ill-posedness is resolved by choosing the homogeneous flow model, and furthermore assuming stationary momentum. This approach has been used by a number of workers in the solar thermal field [57 - 61].

Jance et al [62] discussed about the natural convection and radiation within the enclosed inverted absorber cavity by using numerical simulation. The paper described the development of a test rig for assessing the optimum geometry and thermal efficiency of an insulated enclosure, which surrounds an inverted plate absorber, for a large solar thermal steam generating plant. Smoke was introduced into the cavity, and a sheet of quartz-halogen light is projected across the cavity profile to enable convection cells in the cavity to be visualized. The location of the light sheet is midway along the length of the cavity. A two dimensional model of the experimental rig configuration was entered into a computational fluid dynamic package. A grid consisted of approximately 36000 quadrilateral cells. The boundary conditions are shown in Table 1.

Property	Units	Absorber	Side Walls	Window
Temperature, T	°C	300	Calculated	Calculated
Overall heat loss coefficient, h	W/m <sup>2</sup> K	Calculated	2	2.6
Ambient Temperature, T <sub>is</sub>	°C	-	20	20
Emissivity, ε	-	0.05	0.3	0.9
External Radiation Temperature	°C	20	20	20

Table 1: Boundary conditions for numerical simulation [62]

The results obtained from the first run of the experimental rig (at a 400 mm depth, 0° inclination), yielded the following result. A symmetric pattern has been achieved with four main cells present. The two cells in the lower half of the cavity were the strongest. The smoke was introduced from the side of the cavity at the bottom. Although the introduction of the smoke disrupts the flow, the cells at the bottom were strong enough to return to their original pattern within a short period. The results obtained were comparable to the numerical result, although the plume is not as prominent in the experimental result. Reynolds et al [63] explained combined natural and radiation heat transfer in a trapezoidal cavity absorber. They presented the results of a computational investigation of the thermal performance of the trapezoidal cavity absorber. Fig. 3, shows the schematic diagram of the cavity along with the internal modes of heat loss. A flat plate absorber was enclosed in a trapezoidal cavity, of which it forms the top surface. They have analyzed the cavity depths of 100 mm, 400 mm, and for a 100 mm depth, cavity inclined transversely at 10°. The analysis shows that as the cavity depth increases, the window temperature falls and this causes more radiation losses from the absorber plate to increase since the temperature difference between the absorber and the window increases. The optimal depth increases slightly with increase in the external

convection coefficient on the window. The optimal depth was found to decrease as the emissivity of the absorber surface increases. Radiation losses account for the bulk of the total heat loss from the absorber in all cases considered. Also, inclination of the cavity by up to 10° results in only a slight increase in the overall heat loss from the absorber.

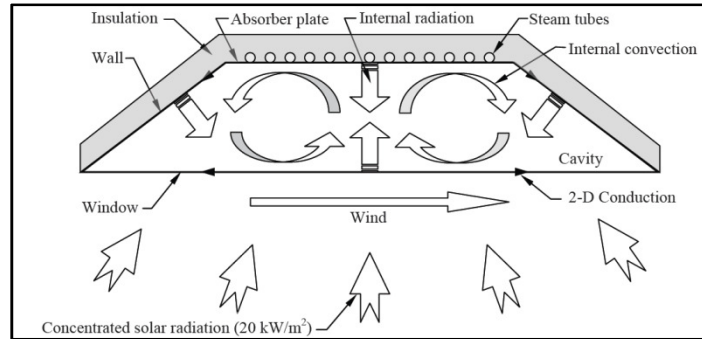


Figure 3: Absorber and cavity arrangement showing modes of internal heat transfer [9]

Reynolds et al [9] developed a hydrodynamic model of line-focus steam generation solar concentrator. Analysis of the heat loss characteristics of the cavity absorber has been conducted, and correlations of the heat loss from the absorber as a function of a number of variables of practical interest have been developed. These correlations have been incorporated into a steady-state hydrodynamic model of the flow through the absorber, including two-phase flow. The model thereby allows prediction of the output steam conditions and pressure drop for given input and environment conditions. Pye et al [7] discussed the development of the cavity absorber by considering the cavity depth and width parameters and new heat loss correlation equations were provided. The computational model with a mesh size of 2 mm was used, following the mesh sensitivity carried out by Reynolds et al [9]. Table 2 and 3 show the values of the fixed and varied parameters respectively that were used to generate the 72 different model cases. From the simulation, they concluded that the optimum depth will be different for the narrower width of  $W = 0.5$  m cavity and suggested that more simulations are required to determine this optimization. So based on previously obtained experimental data for a trapezoidal cavity absorber, CFD models were developed for the purpose of predicting these heat losses, which were the combination of convective, radiative and conductive losses. Also, they made an attempt to develop design correlations for the prediction of heat losses using suitable Nusselt and Grashof numbers for convection, and an effective radiation view factor met with reasonable success.

Constant Parameter	Value
Absorber emissivity in cavity	0.49
Wall emissivity in cavity	0.1
Emissivity of the window (internal and external)	0.9
Operating temperature of the cavity (for Boussinesq approximation)	370 K
Overall external heat loss coefficient on cavity walls	0.5 W/m <sup>2</sup> K

Table 2: Fixed parameters used in the simulations [7]

Constant Parameter	Value
Cavity depth	100, 200 and 300 mm
Cavity width (at top)	500, 1200 mm
Absorber temperature	530, 570, 610 K
Ambient temperature	290, 305 K
Convection coefficient on outside of glass cavity window	2, 6, 10 W/m <sup>2</sup> K

Table 3: Varied parameters used in the simulations [7]

In another paper, Pye et al [64] discussed about the transient modeling of cavity absorber heat transfer. Unsteady flow patterns in the cavity absorber have been investigated by using computational methods. A range of simulations was run to compute the heat transfer from the absorber cavity over a period of time, using the full cavity model, for covering the following domain of parameters: two different cavity widths (0.5 and 1.2 m), three aspect ratios (1:5, 2:5 and 3:5), three absorber temperatures (530 K, 570 K and 610 K), and two external convection coefficients (10 W/m<sup>2</sup> and 25 W/m<sup>2</sup>). Model cases were run for one hour of simulated time using an adaptive time step up of 0.5s. The regression analysis with the full-cavity, unsteady simulation results gave the following,

$$Nu = 0.163Gr^{0.196} \left(\frac{D_e}{w}\right)^{0.316} \tag{2.16}$$

The parameters in this correlation were different from the earlier result [7]. From the correlation, it was identified that the Grashof number has assumed greater importance and the aspect ratio a lesser importance. The reason is that in the previous paper, author [7] gave the broader range of aspect ratios. This form of correlation was different to that used by Reynolds et al [8], in that only intrinsic parameters of the cavity were used for the absorber heat transfer due to convection. Also, he concluded that this correlation (Equation

2.16) is suitable for temperatures on the absorber of 530 K to 610 K, and with convection on the cavity cover between 10 and 25  $\text{W/m}^2$ , for external temperatures from 293 K to 308 K, and for fixed values of emissivity for the various surfaces as given here: absorber emissivity - 0.49, sidewalls emissivity - 0.1, cavity cover emissivity - 0.9. The angle of the sidewalls is  $30^\circ$  from the horizontal. So the above analysis gave a practical way to estimate the cavity heat loss based on more accurate simulations than those previously performed. The correlation for the heat loss from the absorber has been found out and it was similar form to that previously found but applies to a different domain of parameters, which has resulted in altered coefficients in the correlation. Unsteadiness in the flow pattern appeared in the simulation results but its effect on the overall heat loss transfer was small, since the oscillations in total heat transfer occur over a very small range relative to the magnitude of the total heat transfer.

Boussaid et al [65] studied heat and mass transfer problem in a trapezoidal cavity absorber. The top and lower inclined parts of the cavity were considered as heated and cooled part respectively. Using alternating direction implicit (ADI) method, combined with a highly accurate fourth-order Hermitian method, the required heat and mass transfer equations were solved. They concluded that the thermo-convective instabilities obtained are similar to those obtained in rectangular cavities. Reynolds et al [50] examined the heat loss characteristics of a cavity absorber. The cavity was trapezoidal in cross-section and upper surface of the cavity is a flat plate absorber with steam tubes running behind it. They described the experimental techniques to investigate the heat losses from the absorber, and the flow visualization technique to capture the flow pattern within the cavity. Reasonable agreement between the experimentally determined heat losses and those predicted by the FLUENT model has been obtained. The cavity size is 420 mm depth and 1550 mm length. The lower surface of the cavity is 520 mm wide. Three flat 800 W heaters, each  $500 \times 500$  mm in area, were suspended from the upper surface of the cavity to represent the hot absorber plate. Smoke was introduced into the cavity in order to visualize the flow cells inside the cavity. The smoke within the light sheet allows these flows to be seen clearly and photographed. Similarly, a computational model of the prototype absorber has been developed using the FLUENT V.5 commercial CFD software package. The heater surface was modeled as an isothermal surface with a specified temperature of  $300^\circ\text{C}$  and an internal emissivity of 0.10. The sidewalls were modeled as convection boundaries with convection coefficients of  $0.79 \text{ W/m}^2\text{K}$ , exchanging heat with an ambient temperature of  $20^\circ\text{C}$ . The flow in the cavity was modeled as laminar and radiation was modeled using discrete transfer method. Quadrilateral elements were employed with cell size of approximately  $2 \times 2$  mm, with 33,947 mesh point in total. The heat loss predicted by the CFD model was  $623 \text{ W/m}^2$  and experimental result was  $1040 \text{ W/m}^2$  (Fig. 4). So such a thermal model could be used to optimize the thermal efficiency of the absorber cavity and could also be incorporated into a control system for LFR type solar thermal collector.

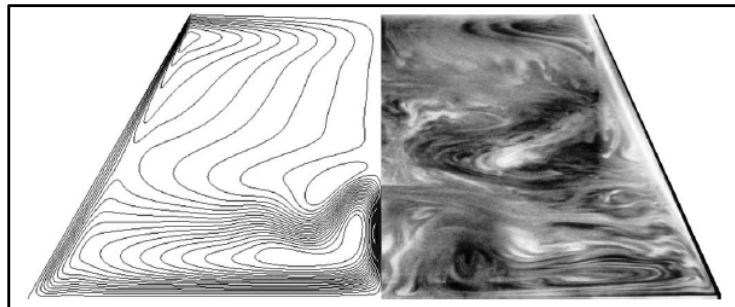


Figure 4: Experimental flow visualization and heat transfer (right) with CFD predictions (left) [50]

Dey [20] studied the heat transfer aspects of an elevated linear absorber for LFRSC system. The design methodology and heat transfer calculations for an elevated north-south oriented linear absorber has been discussed. The basic absorber design used was an inverted air cavity with a glass cover enclosing a selective surface. Two main design aims were discussed, firstly to maximize the heat transfer between the absorbing surface and the steam pipes, and secondly, to ensure that the absorber surface temperature is sufficiently uniform so as not to cause thermal degradation of the selective surface coated absorber at low temperature differences between the fluid surfaces. The absorbing surface ( $< 20 \text{ K}$ ) can be achieved with satisfactory pipe separations and sizes, and with practical absorber plate thickness. Various bar thickness and pipe pitches have been modeled (Fig. 5) for the nominal 15 mm pipe size ( $\sim 22 \text{ mm OD}$ ).

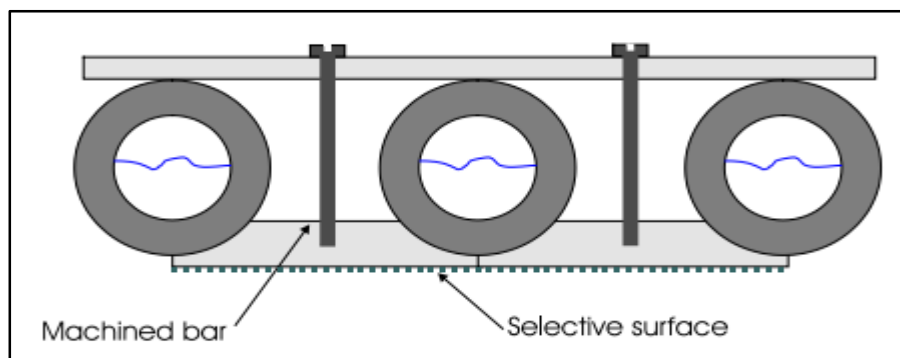


Figure 5: Schematic diagram of the bar absorber design showing the basic arrangements [20]

In all cases the minimum bar thickness is 1 mm, occurring below the center of the pipe. Thicker bars therefore have more material on their upper side, and hence, more contact area with the absorber pipe. For the minimum pipe spacing possible for these pipes, an 8 mm thick plate can ensure a maximum temperature difference of less than 20 K. The results showed that at approximately the closest allowance spacing, bar thickness down to 5 mm can ensure the maximum temperature difference is kept below 20 K. So the results indicated that acceptable  $\Delta T_{\max}$  values (less than 20 K) can be achieved for reasonable bar thickness (~ 6 mm) and for pipe spacing which comply with the relevant standards for pressure equipment.

Hammami et al [65] performed three-dimensional numerical study of coupled heat and mass transfer by natural convection in a trapezoidal cavity using a finite volume technique. Based on these numerical results, thermal and hydrodynamic behavior of the binary mixture air–water vapor system was evaluated. It was observed that as the aspect ratio increased, multi cellular flow patterns were formed. Moukalled & Darwish [66] carried out a numerical study to examine the effects on heat transfer of mounting two offset baffles onto the upper inclined and lower horizontal surfaces of the trapezoidal cavities. Based on the vertical wall in the left and right side of the trapezoidal cavity, two thermal boundary conditions were considered. It was observed that the decrease in heat transfer in the presence of baffles and increasing with increased Pr and baffle height. Tmartnhad et al [67] carried out a numerical study of mixed convection from a trapezoidal cavity. Two openings were adjusted on the plates of the cavity to study the effect of Reynolds number on the heat transfer by mixed convection. Arici & Sahin [65] numerically studied natural convection heat transfer in a partially divided trapezoidal enclosure using a control volume method. Also summer and winter condition heat transfer results were examined in a partially divided trapezoidal enclosure. Kumar & Reddy [69] developed Nusselt number correlations with less number of data points for pure convection and combined natural convection and surface radiation for modified cavity absorber through ACFD (asymptotic computational fluid dynamics) technique and concluded that the heat loss is minimum from the absorber.

Overall heat loss coefficients of the trapezoidal cavity absorber with rectangular and round pipe were studied by Singh et al [22]. In the study, hot oil is used as working fluid and circulated through the cavity absorber tubes at different temperatures. The heat loss coefficient was increased with the absorber temperature. Heat loss in the trapezoidal cavity absorber was also analyzed critically and estimated analytically by parallel plate correlation and cavity correlation and compared with the experimental results. The heat loss coefficients for ordinary black coated and selective surface coated round pipe absorbers varied from 3.5 to 7.5 W/m<sup>2</sup>°C and 2.7 to 5.8 W/m<sup>2</sup>°C respectively. Finally they concluded that the double glass cover was better compared to single glass cover as there was reduction in overall heat loss coefficient by 10 – 15%. No significant difference obtained between overall heat loss coefficient values of rectangular and round pipe absorbers used inside the trapezoidal cavity. The trend of variation of overall heat loss coefficient estimated by parallel plate correlation and cavity correlation were similar to the experimental values. Fig.6 shows the variation of overall heat loss coefficient for selective surface coated rectangular pipe absorber with double cover for parallel plate correlation and cavity correlation with experimental values. The estimated overall heat loss coefficient by the cavity correlations were closure and uniformly distributed for all temperature range. Also, correlation between overall heat loss coefficient and absorber temperature has been developed for experimental data in generalized form as follows

$$U_l = c_l (T_s)^d \quad (2.17)$$

where  $c_l$  and  $d$  are constants and  $T_{\text{abs}}$  is the absorber surface temperature. The correlation has been developed for both rectangular and round pipe absorber with different surface coating. The deviation between experimental and predicted correlated values was within  $\pm 10\%$ .

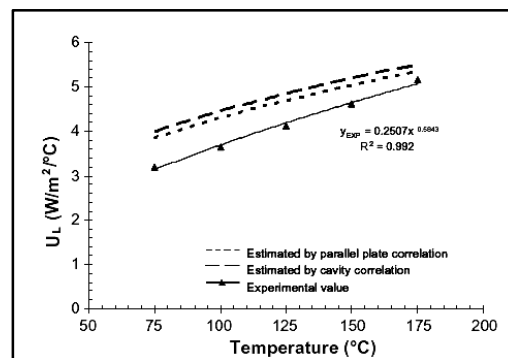


Figure 6: Variation of overall heat loss coefficient [19]

Facao & Oliveria [70] analyzed the optical and thermal performance of a new trapezoidal cavity absorber for a small linear Fresnel solar collector through ray-trace and CFD simulations. Overall heat loss coefficient of the cavity absorber (Natural convection, surface radiation and conduction) was also evaluated. In another work, Facao & Oliveria [71] used CFD simulation to optimize cavity depth and rock wool insulation thickness. It was concluded that the cavity (Table 4) with a 45 mm depth presents the lowest global heat transfer coefficient as compared to 25 and 65 mm. Regarding insulation thickness (Table 5), 35 mm of rock wool presented a good compromise between insulation and shading. Also, the simulated global heat transfer coefficient, based on primary mirror area, was correlated with a power-law fit instead of a parabolic fit.

<b>D<sub>e</sub> [mm]</b>	25	45	65
<b>U<sub>l</sub> [W/m<sup>2</sup>K]</b>	0.2431	0.2383	0.2437
<b>Loss by radiation [%]</b>	65	74	76

Table 4: Influence of receiver depth [70]

<b>T<sub>ins</sub> [mm]</b>	20	35	50
<b>U<sub>l</sub> [W/m<sup>2</sup>K]</b>	0.2545	0.2383	0.2301
<b>Increasing width cavity [%]</b>	30	53	76

Table 5: Influence of insulation thickness [70]

Larsen et al [6] observed the heat loss of a trapezoidal cavity absorber with a set of pipes. The study includes the measurements on a 1.4 m long prototype installed in a laboratory, and its thermal simulation in steady-state using Energy Plus software. Measurements revealed that a stable thermal gradient was in the upper portion of the cavity and a convective zone below it. Around 91% of the heat transferred to outdoors occurs at the bottom transparent window cover, for a pipe temperature of 200°C. Here, they used the simpler and less time consuming available free software (Energy plus) originally designed for heat transfer in buildings was tested to be a possible replacement of the highly complex CFD software commonly used to simulate the steady-state heat loss of the absorber. This factor should be considered in order to improve the thermal efficiency of future designs. Sahoo et al [5] analyzed the steady state modeling and simulation of trapezoidal cavity with eight tubes using CFD. The results obtained by the model were compared with the experimental data. The computations have been carried out for different depths of cavity as well as for different external convective heat transfer coefficients related to different wind speeds near the outer side of glass cover. It has been observed that the dominant mode of heat losses from the cavity is radiation (Fig. 7). Hence, using selective coating on tubes and cavity inside wall, the overall losses can be minimized.

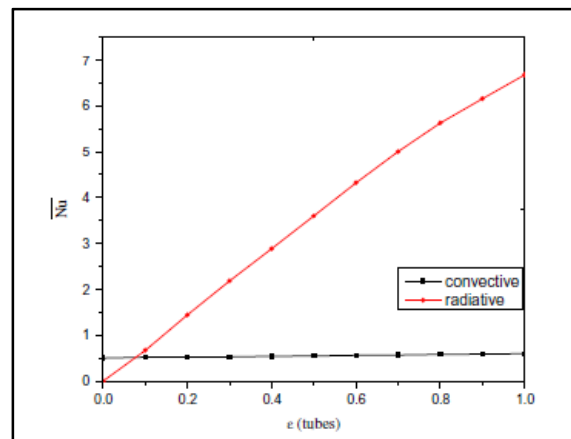


Figure7: Variation of average Nusselt number with the emissivity of the absorber tubes [5].

Although the dominant mode of losses is radiation, the losses by natural convection are also significant. The use of evacuated cavities may be recommended to minimize convection losses. The results from the computational studies were used to obtain correlation between total average Nusselt number and its influencing parameters. Correlations for total average Nusselt number have been proposed for a working fluid of air, whose prandtl number is 0.71.

$$Nu_{cp} = 0.084Ra^{0.19} (T)^{0.53} \left(\frac{1}{D_e}\right)^{0.095} (1 + \epsilon)^{2.292} \left(\frac{h_{ext}W}{K_a}\right)^{0.0304} \tag{2.18}$$

The heat transfer coefficient can be obtained using this correlation for further analysis like fluid flow through the absorber tubes in LFRSC system.

Manikumar et al [26] analyzed computationally the combined natural convection and surface radiation heat transfer from the surface of a trapezoidal cavity absorber of LFRSC system. Two dimensional, Boussinesq, steady state, laminar heat transfer model was developed and analyzed by using the ANSYS workbench with FLUENT. Two different cavity models were considered in the analysis. Former is with absorber plate above which tubes are located and latter is without absorber plate (only absorber tubes) at the top surface of the trapezoidal cavity absorber. The analysis was carried out with the surface painted black and electroplated with nickel black selective surface coating. The correlation between the overall heat transfer coefficient and the absorber temperature for different cavity models were developed. The power-law fit trend line was chosen to correlate to the results. The power curve between heat loss coefficient and absorber temperature was found to be best fit with regression coefficient (R<sup>2</sup>) of about 0.985 on an average. Values of the constant R<sup>2</sup>, c. and d obtained for correlation equation (Eqn. 2.17) for different absorber temperature for the considered models are given in Table 6. The heat loss from the absorber plate found lower compared to the absorber tubes placed directly at the top surface of the cavity. The selective surface coating on the absorbers found to be useful, as compared to ordinary black paint. There was

significant reduction in overall heat loss coefficient (up to 57%) in the latter case. The cavity with absorber plate was useful as compared to absorber tubes directly exposed to solar radiation (as there was reduction in overall heat loss coefficient by 21–25%).

Model	Coating	Analysis type	R <sup>2</sup>	c'	D
Trapezoidal Cavity with absorber plate	Selective surface coating	CFD Simulated	0.999	0.376	0.484
	Black coating	CFD Simulated	0.999	0.335	0.673
Trapezoidal Cavity with absorber tubes	Selective surface coating	CFD Simulated	0.996	0.875	0.445
	Black coating	CFD Simulated	0.99	1.02	0.501

Table 6: Values of the constants R<sup>2</sup>, c' and d obtained for simulated results [26].

**5. Selection of Best Approximation Theory**

One of the great challenges in the design of a cavity absorber using CFD approach is the selection of appropriate model. When CFD simulations of a flow through a cavity absorber are concerned, we often wonder, whether the simulation produces a precise image of the real flow. The question is not answered easily, as the quality of the obtained result depends on many parameters of the computer model [72]. Modern CFD programs offer their users many possible parameters of the mathematical model. For the present model, in most of the literature review there is no separate or combined non-Boussinesq convection and surface radiation heat transfer model for trapezoidal cavity geometry [72&73]. Hence, the low temperature application (<100°C) Boussinesq natural convection and surface radiation heat transfer model for square cavity [37] has been considered to validate with low temperature non-Boussinesq heat transfer model. At lower temperature, the Boussinesq and non-Boussinesq approach give same results. Only at higher temperature, the Boussinesq approximation ( $\Delta\rho/\rho \ll 1$ ) is not valid. By using the non-Boussinesq numerical procedure, the combined natural convection and surface radiation Nusselt number has been predicted for square cavity and compared with the developed Nusselt number correlations for square cavity [37]. To perform this, the Grashof numbers of 104, 105 and 106 and temperature ratio and emissivity of 0.91 and 0.3 have been taken. The predicted combined convective and radiative Nusselt number for the square cavity based on the non-Boussinesq approximation numerical procedure and thecalculated combined Nusselt number based on the square cavity geometry is given in the Table 7. It was observed that the predicted Nusselt number through present numerical procedure agrees well with analytical Nusselt number based on square cavity geometry.

Grashof Number (Gr)	Parameters of square cavity		Combined convective and radiative average Nusselt numbers from the correlations	Combined convective and radiative Nusselt number, based on present numerical procedure	Percentage of deviation
	Average Nusselt Number				
4.8154 * 10 <sup>4</sup>	NuC NuR	3.41 0.97	4.38	4.32	1.36
3.8523 * 10 <sup>5</sup>	NuC NuR	6.33 1.97	8.30	8.23	0.84
1.0670 * 10 <sup>6</sup>	NuC NuR	8.53 2.77	11.31	11.28	0.26

Table 7: Validation of the numerical procedure [37]

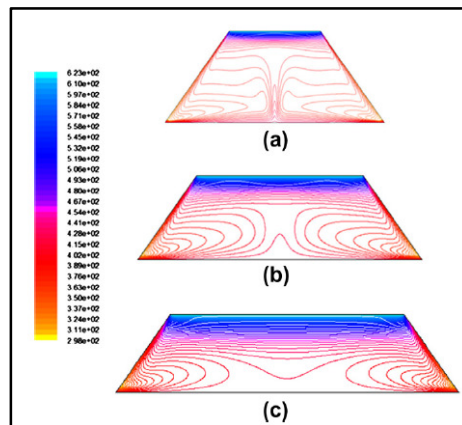


Figure 8: Temperature contours of trapezoidal cavity absorber at different aspect ratio (a) W/De = 1; (b) W/De = 2 (c) W/De = 3 [28]

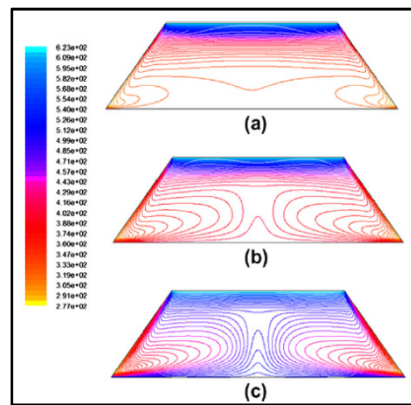


Figure 9: Temperature contours of trapezoidal cavity absorber at different temperature ratio (a)  $T_c/T_p = 0.15$ ; (b)  $T_c/T_p = 0.45$ ; and (c)  $T_c/T_p = 0.75$  [28]

Natarajan et al [28] studied the heat loss characteristics in the cavity absorber. The CFD package, FLUENT 6.3 was used to develop the 2-D, non-Boussinesq, steady state, laminar, combined natural convection and surface radiation heat transfer model for a trapezoidal cavity absorber. Based on this model, a combined natural convection and surface radiation Nusselt number correlation were proposed. It was found that the effect of combined Nusselt number on trapezoidal cavity side wall angle is negligible. Beyond the aspect ratio (Fig. 8) of 2.5 and temperature ratio (ratio between the bottom and top surface temperatures of the cavity) of 0.6 (Fig. 9), the variation of combined heat loss in trapezoidal absorber is not significant. The trapezoidal cavity absorber with aspect ratio and temperature ratio of greater than 2.5 and 0.6 respectively can be used to minimize the internal heat loss of the absorber. They concluded that by using non-Boussinesq approximation model, the heat loss at high absorber temperature can be predicted accurately. Manikumar et al [27] discussed the models by comparing Boussinesq and non-Boussinesq approximations in numerical simulation study.

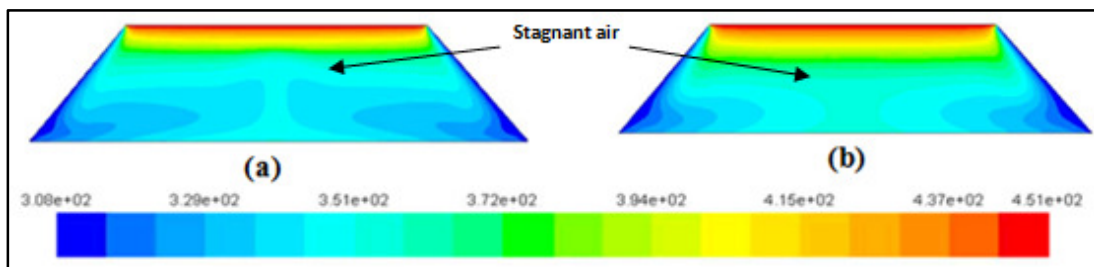


Figure 10: Temperature contours of trapezoidal cavity with plate at  $178^\circ\text{C}$  for ordinary black paint coating (a) Boussinesq approximation (b) non-Boussinesq approximation [27].

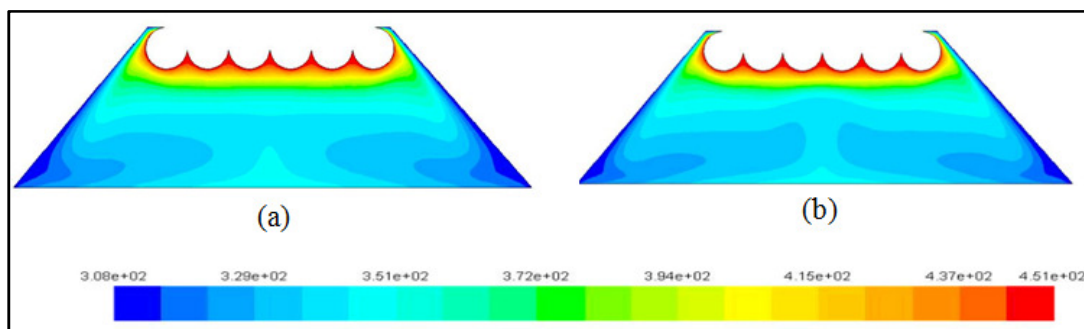


Figure 11: Temperature contours of trapezoidal cavity without plate at  $178^\circ\text{C}$  for ordinary black paint coating (a) Boussinesq approximation (b) non-Boussinesq approximation [27].

It was found that, for all the considered surface temperatures, the thickness of the stagnant air zone near the top of the cavity is more in the cavity with non-Boussinesq approximation as compared to that of Boussinesq approximation (Fig. 10 (a) and (b)). Increasing the thickness of the stagnant air correspondingly decreases the combined heat loss in a trapezoidal cavity and thus it was inferred that, the numerical simulation technique by using non-Boussinesq approximation gives better results as compared to Boussinesq approximation. Also, it was observed that the thickness of the stagnant air zone near the top surface was more in cavity with plate compared to that of cavity without plate (Fig. 10 and Fig. 11). This also leads to reduction of combined heat loss in a trapezoidal cavity with plate. The trend of variation of overall heat loss coefficient estimated with non- Boussinesq approximations was similar to that of analytical and experimental values. Also, the simulated values predicted by using non-Boussinesq approximation were close to

analytical and experimental values. Good agreement between predicted (numerical and analytical simulated) values and experimental values were observed (within 10%).

A number of historical and current absorber models related to LFRSC were reviewed. The efficiency of the LFRSC plant is mainly determined by the amount of energy collection at the cavity absorber that is the subject of the present review work. Several numerical simulated results validated with analytical and experimental results have been presented to explain the phenomenon of combined natural convection and surface radiation in a closed cavity. Various ways of research work were discussed related to this technique. Also, various computational techniques like CFD, Energy Plus software etc., have been used for the modeling and heat loss analysis of the cavity absorber. Finally it can be concluded that non-Boussinesq approximation (considering density variation with high temperature) theory predicts very close results to the experimental results, which yields confidence in the predictions done by CFD analysis in the design of a cavity absorber.

## 6. Conclusion

This article presents a detailed review of the literature that deals with the application of CFD in design of cavity absorber for a LFRSC system. In this article a CFD investigation is carried out to select best approximation model for the design of a cavity absorber. A modern CFD code ANSYS FLUENT is used to simulate heat transfer and fluid flow through a cavity absorber. A two-dimensional flow is assumed. The influences of the Boussinesq and non-Boussinesq approximation models on the quality of the obtained results are tested. On the basis of the review of the literature and CFD investigation of cavity absorber, the conclusion can be summarized as follows:

1. The present literature review reveals that a few studies have been done on CFD analysis of heat transfer in a cavity absorber.
2. Major focus of CFD simulation of cavity absorber is to enhance the heat transfer and fluid flow analysis.
3. CFD simulation results are found to be in good agreement with experimental results and with the standard theoretical approaches. Although there are some small discrepancies due to some experimental imperfectness matters, we still have a good confidence in the CFD simulation that can be used in the future for more complex geometry of cavity absorber.
4. The quality of the solutions obtained from CFD simulations are largely within the acceptable range proving that CFD is an effective tool for predicting the behavior and performance of a cavity absorber.
6. In summary, the purpose of this article is to illustrate the use of CFD in analysis of heat transfer in cavity absorber of a LFRSC system and to use this to indicate the wide open future of CFD design. No matter how mature the techniques of CFD may become, the array of future and challenging applications of CFD is limitless. There is tremendous scope for future study of various models of cavity absorber with CFD approach. The information presented here will be useful and beneficial for beginners in this area of research. Authors hope that this article has opened the horizons of CFD analysis of cavity absorber to researchers in LFRSC system.

## 7. Nomenclatures

$A_a$	-	Aperture area of the concentrator [ $m^2$ ]
$A_p$	-	Absorber plate area [ $m^2$ ]
$A_r$	-	Absorber tubes surface area [ $m^2$ ]
$C$	-	Constant used to find Nusselt number
$c$	-	Specific heat of the water [ $kJ/kgK$ ]
$D_e$	-	Distance between the absorber surface and transparent cover [ $mm$ ]
$F'$	-	Collector efficiency factor
$Gr$	-	Grash of number
$g_r$	-	Gravity [ $m/s^2$ ]
$h_{co}$	-	Convection heat loss coefficient from the bottom glass surface [ $W/m^2-K$ ]
$h_{cp}$	-	Convection heat loss coefficient from the absorber surface [ $W/m^2-K$ ]
$h_{ext}$	-	External heat loss coefficient [ $W/m^2-K$ ]
$h_{ro}$	-	Radiation heat loss coefficient from the bottom glass surface [ $W/m^2-K$ ]
$h_{rp}$	-	Radiation heat loss coefficient from the absorber surface [ $W/m^2-K$ ]
$h_w$	-	Heat loss coefficient from the transparent cover to the surroundings [ $W/m^2-K$ ]
$I$	-	Direct component of solar flux [ $kW/m^2$ ]
$k_a$	-	Thermal conductivity of air [ $W/m^2-K$ ]
$m$	-	mass flow rate of the fluid [ $kg/s$ ]
$N$	-	Total number of reflector on either side of the central reflector of the concentrator.
$Nu_{cp}$	-	Nusselt number
$Nu_C$	-	Convective Nusselt number
$Nu_R$	-	Radiative Nusselt number
$P$	-	Pressure [ $N/m^2$ ]
$P_i$	-	Pitch distance between the absorber tubes [ $mm$ ]
$q_i$	-	Energy flux incident on the surface from the surrounding [ $W/m^2$ ]
$q_l$	-	Heat lost from the absorber surface [ $W$ ]
$q_o$	-	Energy flux leaving the surface [ $W/m^2$ ]
$q_u$	-	Useful heat gain [ $W$ ]

R	-	Location of constituent mirror elements [m]
Ra	-	Rayleigh number
S	-	Absorbed flux [W/m <sup>2</sup> ]
T	-	Temperature of the working fluid [°C]
T <sub>a</sub>	-	Ambient temperature [°C]
T <sub>c</sub>	-	Cover temperature [°C]
T <sub>fi</sub>	-	Fluid outlet temperature [°C]
T <sub>fo</sub>	-	Fluid outlet temperature [°C]
T <sub>i</sub>	-	Water inlet temperature [°C]
T <sub>ins</sub>	-	Insulation thickness [mm]
T <sub>o</sub>	-	Water outlet temperature [°C]
T <sub>p</sub>	-	Absorber plate temperature [°C]
T <sub>s</sub>	-	Absorber tube surface temperature [°C]
U <sub>l</sub>	-	Overall heat loss coefficient [W/m <sup>2</sup> K]
u	-	Velocity at x-coordinates [m/s]
V <sub>w</sub>	-	Velocity of the wind [m/sec]
v	-	Velocity at y-coordinates [m/s]
w	-	Width of the reflector [m]
W	-	Width of the absorber plane [m]

#### Greek Symbols

$\mathcal{E}$	-	Half of the angular subtense of the sun at any point on the earth [=16']
$\mathcal{E}_p$	-	Emissivity of the absorber surface
$\mathcal{E}_c$	-	Emissivity of the transparent cover
$\sigma$	-	Stefan Boltzman constant [5.67X10 <sup>-8</sup> W/m <sup>2</sup> -K <sup>4</sup> ]
$\rho_f$	-	Density of the working fluid [kg/m <sup>3</sup> ]
$\mu$	-	Dynamic viscosity [kg-m/s]
$\mu_n$	-	Dynamic viscosity corresponding to various absorber surface temperatures [kg-m/s]
$\mu_o$	-	Reference dynamic viscosity [kg-m/s]
$\eta$	-	Thermal efficiency [%]

#### 8. References

- i. Singh, PL, Sarviya, RM & Bhagoria, JL 2010a, 'Thermal performance of linear Fresnel reflecting solar concentrator with trapezoidal cavity absorbers', Applied Energy, vol. 87, pp. 541-550.
- ii. Babu, M & Valan Arasu, A 2015, 'Theoretical Performance analysis of linear Fresnel reflector concentrating solar system with horizontal absorber', Australian Journal of Basic and Applied Sciences, vol. 9 (27), pp. 101-111.
- iii. Babu, M & Valan Arasu, A 2015, 'Theoretical Performance analysis of linear Fresnel reflector concentrating solar system with vertical absorber', Australian Journal of Basic and Applied Sciences, vol. 9 (20), pp. 473-484.
- iv. Babu, M & Valan Arasu, A 2015, 'Performance analysis of linear Fresnel reflector concentrating solar system with varying reflector width using analytical and ray tracing techniques', Progress in Industrial Ecology – An International Journal, vol. 9 (2), pp. 121-134.
- v. Sudhansu Sahoo, S, Suneet Singh & Rangan Banerjee 2012, 'Analysis of heat losses from a trapezoidal cavity used for Linear Fresnel Reflector system', Solar Energy, vol. 86, pp. 1313-1322.
- vi. Flores Larsen, S, Altamirano, A & Hernandez, A 2012, 'Heat loss of a trapezoidal cavity absorber for a linear Fresnel reflecting solar concentrator', Renewable Energy, vol. 31, pp. 198-206.
- vii. Pye, JD, Morrison, GL, Behnia, M & Mills, D 2003 a, 'Modelling of cavity receiver heat transfer for the compact linear Fresnel reflector', Proceedings of ISES Solar World Congress 2003 - Solar Energy for a Sustainable Future, Gothenburg, Sweden.
- viii. Reynolds, DJ, Behnia, M & Morrison, GL 2002, 'A hydrodynamic model for a line-focus direct steam generation solar collector', in Proceedings of Solar 2002, Australian and New Zealand Solar Energy Society.
- ix. Manikumar, R & Valan Arasu, A 2012, 'Design and theoretical performance analysis of linear Fresnel reflector solar concentrator with single tube absorber', International Journal of Renewable Energy Technology, Inderscience Publication, vol. 3, no. 3, pp. 221-236.
- x. Anil Singh Yadav & Bhagoria, JL 2013, 'Heat transfer and fluid flow analysis of solar air heater: A review of CFD approach', Renewable and Sustainable Energy Reviews, Sciverse Science Direct, vol. 23, pp. 60-79.
- xi. Date AW. Introduction to computational fluid dynamics. 1st ed.. New York: Cambridge University Press; 2005.
- xii. Chung TJ, editor. Cambridge UK: Cambridge University Press; 2002.
- xiii. Cebeci T, Kafyke F, Shao JP, Laurendeau E. Computational fluid dynamics for engineers. 1st ed.. New York: Springer; 2005.
- xiv. Ferziger JH, Peric M. Computational method for fluid dynamics. 3rd ed.. New York: Springer; 2002.

- xv. Blazek J. Computational fluid dynamics—principles and applications. 1st ed.. Oxford, UK: Elsevier; 2001.
- xvi. Garg HP, Prakash J. Solar energy fundamentals and applications. 1st ed.. New Delhi: Tata McGraw-Hill; 2000.
- xvii. Sukhatme, SP & Nayak, JK 2009, Solar energy principles of thermal collection and storage, Tata McGraw-Hill Publication, New York.
- xviii. Kalogirou, S 2004, 'Solar thermal collectors and applications progress in energy and combustion science', vol.30, pp. 231-295.
- xix. Duffie, JA & Beckman, WA 1991, Solar Engineering of thermal process, John Wiley, New York.
- xx. Dey, CJ 2004, 'Heat transfer aspect of an elevated linear absorber', Solar Energy, vol. 76, pp. 243-249.
- xxi. Chapman, A.J. 1984. Heat transfer. New York: Macmillan.
- xxii. Singh, PL, Sarviya, RM & Bhagoria, JL 2010b, 'Heat loss study of trapezoidal cavity absorbers for linear solar concentration collector', Energy Conversion and Management, vol. 51, pp. 329-33.
- xxiii. Patankar SV. Numerical heat transfer and fluid flow. 1st ed.. USA: Hemisphere Publishing Corporation; 1980.
- xxiv. Tannehill JC, Anderson DA, Pletcher RH. Computational fluid mechanics and heat transfer. 2nd ed.. London: Taylor & Francis; 1997.
- xxv. FLUENT. 2009. ANSYS workbench, FLUENT 12.0 user's guide. 2009. Canonsburg, PA: ANSYS Inc.
- xxvi. Manikumar, R, Valan Arasu, A & Jayaraj, S 2013, 'Numerical simulation of a trapezoidal cavity absorber in the linear Fresnel reflector solar concentrator system', Int. J. of Green Energy, Taylor and Francis, vol. 11, 344 – 363, 2014.
- xxvii. Manikumar, R, Valan Arasu, A & Jayaraj, S 2012, 'Computational fluid dynamics analysis of a trapezoidal cavity absorber used for the linear Fresnel reflector solar concentrator system', Journal of Renewable and Sustainable Energy, American Institute of Physics, vol. 4, no. 6, pp. 063145 (1-18).
- xxviii. Sendhil Kumar Natarajan, Reddy, KS & Tapas Kumar Mallick 2012, 'Heat loss characteristics of trapezoidal cavity receiver for solar linear concentrating system', Applied Energy, vol. 93, pp. 523-531.
- xxix. Reynolds, DJ, Janes, MJ, Behina, M & Morrison, GL 2004, 'An experimental and computational study of the heat loss characteristics of a trapezoidal cavity absorber', Solar Energy, vol. 76, pp. 229-234.
- xxx. Kim, DM & Viskanta, R 1984, 'Heat transfer by conduction, natural convection and radiation across a rectangular cellular structure', International Journal of Heat and Fluid Flow, vol. 5, no. 4, pp. 205-213.
- xxxi. Nakamura, H & Asako, Y 1984, 'Combined free convection and radiation heat transfer in rectangular cavities with a partition wall', Trans. JSME B, vol. 50, no. 459, pp. 2647-2654.
- xxxii. Fusegi, T & Farouk, B 1989, 'Laminar and turbulent natural convection radiation interactions in a square enclosure filled with a non gray gas', Numerical heat transfer - Part A, vol. 15, pp. 303-322.
- xxxiii. Fusegi, T & Farouk, B 1990, 'A computational and experimental study of natural convection and surface/gas radiation interactions in a square cavity', Journal of heat transfer, vol. 112, pp. 802-804.
- xxxiv. Behnia, M, Reizes, JA, & De Vahl Davis, G 1985, 'Natural Convection in a Rectangular Slot With Convective – Radiative Boundaries', ASME National Heat Transfer Conference, Denver, Colorado.
- xxxv. Balaji, C & Venkateshan, S 1993, 'Interaction of surface radiation with free convection in a square cavity', International Journal of Heat and Fluid Flow, vol. 14, no. 3, pp. 260-267.
- xxxvi. Tong, W & Koster, JN 1993, 'Natural convection of water in a rectangular cavity including density inversion', International Journal of Heat and Fluid Flow, vol. 14, no. 4, pp. 366-375.
- xxxvii. Balaji, C & Venkateshan, S 1994, 'Correlation for free convection and surface radiation in a square cavity', International Journal of Heat and Fluid Flow, vol. 15, pp. 249-51.
- xxxviii. Mlaouah, H, Tsuji, T & Nagano, Y 1997, 'A study of non-Boussinesq effect on transition of thermally induced flow in a square cavity', Int. J. Heat Fluid Flow, vol. 18, pp. 100-106.
- xxxix. Cheng, X & Muller, U 1998, 'Turbulent natural convection coupled with thermal radiation in large vertical channels with asymmetric heating', Int. J. Heat Mass Transfer, vol. 41, no. 12, pp. 1681-1692.
- xl. Ramesh, N & Venkateshan, SP 1999, 'Effect of surface radiation on natural convection in a square enclosure', Journal of Thermophysics and Heat Transfer, vol. 13, no. 3, pp. 299-301.
- xli. Mezrhab, A & Bchir, L 1999, 'Radiation-natural convection interactions in partitioned cavities', International Journal Numerical Methods of Heat and Fluid Flow, vol. 9, no. 2, pp. 186-203.
- xl.ii. Han, CY & Baek, SW 2000, 'The effects of radiation on natural convection in a rectangular enclosure divided by two partitions', Numerical Heat Transfer – part A, vol. 37, pp. 249-270.
- xl.iii. Vierendeels, J, Merci, B & Dick, E 2001, 'Numerical study of natural convective heat transfer with large temperature differences', International Journal of Numerical Method, vol. 11, no. 4, pp. 329-341.
- xl. iv. Mezrhab, A, Bouali, H & Abid, C 2005, 'Modelling of combined radiative and convective heat transfer in an enclosure with a heat-generating conducting body', Int. J. Comput. Methods, vol. 2, No. 3, pp. 431-450.
- xl. v. Bouali, H, Mezrhab, A, Amaoui, H & Bouzidi, M 2006, 'Radiation—natural convection heat transfer in an inclined rectangular enclosure', International Journal of Thermal Sciences, vol. 45, pp. 553-566.
- xl. vi. Manikumar, R & Valan Arasu, A 2014, 'An analytical and experimental study of the linear Fresnel reflector solar concentrator system', Distributed Generation and Alternative Energy, Taylor and Francis, vol. 2 (2), pp. 52-80.
- xl. vii. Gungor, KE & Winterton, RHS 1986, 'A general correlation for flow boiling in tubes and annuli', International Journal of Heat and Mass Transfer, vol. 29, no. 3, pp. 351-358.

- xlvi. Stephan, K 1992, Heat transfer in condensation and boiling, Springer, English edition, Translated from 1988 German version. [1992].
- xlix. Odeh, SD 1999, Direct steam generation collectors for solar electric generation systems, Ph.D. thesis, University of New South Wales, Australia.
1. Reynolds, DJ, Janes, MJ, Behina, M & Morrison, GL 2004, 'An experimental and computational study of the heat loss characteristics of a trapezoidal cavity absorber', Solar Energy, vol. 76, pp. 229-234.
  - ii. Liu, Z & Winterton, RHS 1991, 'A general correlation for saturated and subcooled flow boiling in tubes and annuli, based on a nucleate pool boiling equation', International Journal of Heat and Mass Transfer, vol. 34, no. 11, pp.2759-2766.
  - iii. Gungor, KE & Winterton, RHS 1986, 'A general correlation for flow boiling in tubes and annuli', International Journal of Heat and Mass Transfer, vol. 29, no. 3, pp. 351-358.
  - liii. Kandlikar, SG 1990, 'A general correlation for saturated two-phase flow boiling heat transfer inside horizontal and vertical tubes', Journal of Heat Transfer, vol. 112, pp. 219-228.
  - liv. John Lienhard H(V) & John Lienhard, H(IV) 2006, A heat transfer textbook, Phlogiston Press, Massachusetts, 3<sup>rd</sup> edition, Cambridge.
  - lv. Kothandaraman CP & Subramanyan S. Heat and Mass Transfer Data Book. NewDelhi: New Age International Publishers; 2008.
  - lvi. Bruce Stewart, H and BurtonWendroff 1984, 'Two-phase flow: models and methods', Journal of Computational Physics, vol. 56, no. 3, pp. 363-409.
  - lvii. Dagan, E, Muler, M & Lippke, F 1992, 'Direct steam generation in the parabolic trough collector', in Technical report, Plataforma Solar de Almeria-Madrid.
  - lviii. Tobias Hirsch, Markus Eck. & Wolf-Dieter Steinmann 2005, 'Simulation of transient two-phase flow in parabolic trough collectors using Modelica', in proceedings of the 4<sup>th</sup> international Modelica conference, ed. Gerhard Schmitz, Hamburg, pp. 403 – 412.
  - lix. Tobias Hirsch and Markus Eck 2006, 'Simulation of the start-up procedure of a parabolic trough collector field with direct solar steam generation', in Proceedings 5<sup>th</sup> International Modelica Conference, Wien, Osterreich, pp. 135-143.
  - lx. Lippke, F 1996, 'Direct steam generation in parabolic trough solar power plants: numerical investigation of the transients and the control of a once-through system', Journal of Solar Energy Engineering, vol. 118, pp. 9-13.
  - lxi. Muller, M 1991, 'Test loop for research on direct steam generation in parabolic trough power plants', Solar Energy Matter, vol. 24, pp. 222-230.
  - lxii. Jance, MJ, Morrison, GL & Behnia, M 2000, 'Natural convection and radiation within an enclosed inverted absorber cavity, preliminary experimental results', in International Renewable Energy Transforming Business: Proceedings of Solar. Brisbane, ANZSES.
  - lxiii. Reynolds, DJ, Graham Morrison L & Behina, M 2001, 'Combined radiation and natural convection in a trapezoidal cavity absorber', in Proceedings of 7<sup>th</sup> Australasian Heat and Mass Transfer Conference, Townsville.
  - lxiv. Pye, JD, Morrison, GL & Behnia, M 2003 b, 'Transient modeling of cavity receiver heat transfer for the compact linear Fresnel reflector', in ANZSES Solar 2003, Melbourne.
  - lxv. Hammami, M, Mseddi, M, & Baccar, M 2007, 'Numerical study of coupled heat and mass transfer in a trapezoidal cavity', Eng. Appl. Computational Fluid Mechanics, vol. 1, no. 3, pp. 216-226.
  - lxvi. Moukalled, F & Darwish, M 2007, 'Buoyancy induced heat transfer in a trapezoidal enclosure with offset baffles', Numer. Heat Transfer A – Appl., vol. 52, no. 4, pp. 337-355.
  - lxvii. Tmartnhad, I, El Alami, M, Najam, M & Oubarra, A 2008, 'Numerical investigation on mixed convection flow in a trapezoidal cavity heated from below', Energy Convers. Manage, vol. 49, no. 3, pp. 3205-3210.
  - lxviii. Arici, ME & Sahin, B 2009, 'Natural convection heat transfer in a partially divided trapezoidal enclosure', Thermal Science, vol. 13, no. 4, pp. 213-220.
  - lxix. Kumar, NS & Reddy, KS 2010, 'Investigation of convection and radiation heat losses from modified cavity receiver of solar parabolic dish using asymptotic computational fluid dynamics', Heat Transfer Engg., vol. 31, no. 7, pp. 597-607.
  - lxx. Facao Jorge and Armando Oliveria, C 2010, 'Numerical simulation of a linear Fresnel solar collector concentrator', 8<sup>th</sup> International Conference on Sustainable Energy Technologies, Aachen, Germany, pp. 1-6.
  - lxxi. Facao Jorge and Armando Oliveria, C 2011, 'Numerical simulation of a trapezoidal cavity receiver for a linear Fresnel solar collector concentrator', Renewable Energy, vol. 36, pp. 90-96.
  - lxxii. Manikumar, R & Valan Arasu, A 2013, 'Heat loss characteristics study of a trapezoidal cavity absorber with and without plate for a linear Fresnel reflector solar concentrator system', Renewable Energy, Elsevier, vol. 63, pp. 98-108.
  - lxxiii. Manikumar, R, Palanichamy R & Valan Arasu, A 2015, 'Heat Transfer Analysis of an Elevated Linear Absorber with Trapezoidal Cavity in the Linear Fresnel Reflector Solar Concentrator System', Journal of Thermal Science, Springer, vol. 24 (1), pp. 90-98.